DMD Fast Forward. Published on August 16, 2018 as DOI: 10.1124/dmd.118.083014
This article has not been copyedited and formatted. The final version may differ from this version.

SHORT COMMUNICATION

Mouse hepatomas with *Ha-ras* and *B-raf* mutations differ in mitogen-activated protein kinase signaling and response to constitutive androstane receptor activation

Albert Braeuning, Ferdinand Kollotzek, Eva Zeller, Thomas Knorpp, Markus F. Templin, Michael Schwarz

University of Tübingen, Dept. of Toxicology, Wilhelmstr. 56, 72074 Tübingen, Germany (A.B., F.K., E.Z., M.S.); Natural and Medical Sciences Institute, Markwiesenstr. 55, 72770 Reutlingen, Germany (T.K., M. F. T.); German Federal Institute for Risk Assessment, Dept. Food Safety, Max-Dohrn-Str. 8-10, 10589 Berlin, Germany (A.B.)

Running title: CAR activation in *Ha-ras*- and *B-raf*-mutated mouse hepatoma

Corresponding author: Albert Braeuning, German Federal Institute for Risk Assessment, Dept. Food Safety, Max-Dohrn-Str. 8-10, 10589 Berlin, Germany; phone: +49-(0)30-18412-3758; fax: +49-(0)30-18412-63758; email: Albert.Braeuning@bfr.bund.de

Number of text pages: 13
Number of tables: 0
Number of figures: 2
Number of references: 27
Number of words (abstract): 177
Number of words (introduction): 303
Number of words (discussion): 498

List of non-standard abbreviations: APC, adenomatous polyposis coli; CAR, constitutive androstane receptor; CYP, cytochrome P450; DEN, diethylnitrosamine; ERK, extracellular signal-regulated kinase; GS, glutamine synthetase; JNK, Jun N-terminal kinase; MAPK, mitogen-activated protein kinase; MEK, mitogen-activated protein kinase kinase; PB, phenobarbital; RSK, ribosomal S6 kinase

DMD Fast Forward. Published on August 16, 2018 as DOI: 10.1124/dmd.118.083014
This article has not been copyedited and formatted. The final version may differ from this version.

Abstract

Nuclear receptors mediate the hepatic induction of drug-metabolizing enzymes by xenobiotics. Not much is known about enzyme induction in liver tumors. Here, we treated tumor-bearing mice with phenobarbital, an activator of CAR (constitutive androstane receptor), to analyze the response of chemically induced *Ha-ras*- and *B-raf*-mutated mouse liver adenoma to CAR activation *in vivo*. Both tumor sub-populations possess almost identical gene expression profiles. CAR target induction in the tumors was studied at the mRNA and protein levels, and a reverse-phase protein microarray approach was chosen to characterize important signaling cascades. CAR target gene induction was pronounced in *B-raf*-mutated, but not in *Ha-ras*-mutated tumors. Phosphoproteomic profiling revealed that phosphorylated activated extracellular signal-regulated kinase (ERK) 1/2 was more abundant in *Ha-ras*-mutated than in *B-raf*-mutated tumors. ERK activation in tumor tissue was negatively correlated with CAR target induction. ERK activation is known to inhibit CAR-dependent transcription. In summary, profound differences exist between the two closely related tumor subpopulations with respect to the activation of mitogenic signaling cascades, and these dissimilarities might explain the differences in xenobiotic induction of CAR target genes.

Introduction

Juvenile mice treated with the genotoxin diethylnitrosamine (DEN; *N*,*N*-diethylnitrous amide) develop liver tumors with activated mitogen-activated protein kinase (MAPK) signaling, a major driver of proliferation and survival, due to mutations in *Ha-ras* or *B-raf* (Aydinlik et al. 2001; Jaworski et al. 2005; Moennikes et al. 2000). Mouse hepatoma with mutant activated Ha-ras or B-raf exhibit strikingly similar transcriptomic and proteomic profiles; characterized e.g. by a lack of glutamine synthetase (GS) and drug-metabolizing enzymes from the cytochrome P450 (CYP) family (Jaworski et al. 2007; Loeppen et al. 2005; Rignall et al. 2009; Unterberger et al. 2014).

The nuclear receptor CAR is activated by phenobarbital (PB; 5-ethyl-5-phenyl-1,3-diazinane-2,4,6-trione), certain polychlorinated biphenyls, pesticides, or others (Hernandez et al. 2009; Knebel et al. 2018; Oshida et al. 2015). CAR activation provokes tumor promotion, transient hepatocyte proliferation, hepatocyte hypertrophy, and transcriptional induction of drug-metabolizing enzymes, especially CYP2B and CYP2C (Elcombe et al. 2014; Kobayashi et al. 2015; Molnar et al. 2013; Wada et al. 2009). Induction of drug metabolism by xenobiotics has a major impact on the pharmaco- and toxicokinetics of foreign compounds (Tannenbaum and Sheehan 2014).

MAPK activation comprises the activating phosphorylation of extracellular signal-regulated kinase (ERK) downstream of Ha-ras and B-raf (Rubinfeld and Seger 2005). ERK is the most widely used marker for MAPK activation. This potentially links MAPK activation in tumors and CAR activity: nuclear translocation of CAR involves a dephosphorylation step mediated by protein phosphatase 2A (Mutoh et al. 2013), and ERK activation in liver cells diminishes the inducibility of CAR downstream targets by retaining the receptor in the cytosol (Koike et al. 2007). Mutational MAPK activation might thus render tumor cells insensitive to exogenous stimulation of drug-metabolizing enzymes via CAR. Here, we conducted a study with PB treatment of tumor-bearing mice to analyze the responsiveness of *Ha-ras*- and *B-raf*-mutated mouse liver tumors to CAR activation *in vivo*.

Materials and Methods

Animal experiment

Mouse strain, treatment and dosing were based on previous studies demonstrating the induction of MAPK-activated tumors by DEN (Aydinlik et al. 2001; Jaworski et al. 2005; Moennikes et al. 2000). Male mice were selected because of easier tumor induction. Twenty-five C3H/HeN wildtype mice (Charles River, Sulzfeld, Germany) received a single intraperitoneal injection of 10 µg/g body weight DEN (in 0.9% sterile NaCl) at 2 weeks of age. Mice received standard feed (Ssniff, Soest, Germany) and tap water ad libitum. Six months later, mice received 0.05% (w/w) PB via the diet (Ssniff) for 4 weeks. Mice were killed by cervical dislocation between 9 and 11 a.m. to avoid circadian variation; livers were excised, weighed and either immediately frozen on dry ice or fixed in Carnoy's fixative. Animals received humane care and the experimental protocol was approved by a local ethics commission. Tumor samples from non-PB-treated mice, obtained following the identical DEN protocol, were available from previous studies (Jaworski et al. 2005; Moennikes et al. 2000).

Immunohistochemical staining

Formalin-fixed 10 µm cryosections (20 µm for mutation analysis) or 5 µm sections of paraffin-embedded, Carnoy-fixed tissue were stained using standard methods and antibodies against GS (Sigma #G2781; 1:1,000 dilution), E-cadherin (CDH1; BD #610181; 1:100), CYP2B (gift by Dr. R. Wolf, Dundee, UK; 1:300), phosphorylated (pT202/Y204) ERK1/2 (Cell Signaling #4376; 1:100), or 5'-bromodeoxyuridine (BrdU; Dako #M0744; 1:50) as previously described (Braeuning and Schwarz 2010; Braeuning et al. 2010). Nuclei were counterstained using hematoxylin. Images were acquired using a Zeiss Axio Imager microscope (Zeiss, Jena, Germany). Grading of ERK1/2 and CYP2B was performed by microscopic examination of stained slices.

Mutation analysis

Samples were punched out using a sharpened cannula as previously described (Braeuning et al. 2014). Following proteinase K digestion, mutation analyses of codon 61 of *Ha-ras* and codon 637 of *B-raf* were performed using PCR amplification of DNA in combination with restriction fragment length polymorphism analysis as described recently (Braeuning et al. 2014).

Gene expression

Total RNA was extracted using Trizol (Invitrogen, Karlsruhe, Germany) and cDNA was prepared from 375 ng of RNA by avian myeloblastosis virus reverse transcriptase (Promega, Mannheim, Germany). Real-time gene expression analysis on a capillary-based LightCycler was performed using the Fast Start DNA Master^{PLUS} SYBR Green I kit (Roche, Mannheim, Germany). Primers: Cyp2b10 fwd 5'-TACTCCTATTCCATGTCTCCAAA-3', Cyp2b10 rev 5'-TCCAGAAGTCTCTTTTCACATGT-3'; Cyp2c fwd (recognizing multiple Cyp2c isoforms) 5'-CTCCCTCCTGGCCCCAC-3', Cyp2c rev 5'-GGAGCACAGCTCAGGATGAA-3'; Gstm2 fwd 5'-TGGAACCCAAAGTAGGATTACAAA-3', Gstm2 rev 5'-TGAGGACCAAGGCAGCACAC-3'; Gstm3 fwd 5'-GCACTGTGGCTCCCGGT-3', Gstm3 rev 5'- AGGCCTGGGGCAGCTCC-3'; 18S rRNA fwd 5'-CGGCTACCACATCCAAGGAA-3', 18S rRNA rev 5'-GCTGGAATTACCGCGGCT-3'. Expression was calculated relative to 18S rRNA expression according to (Pfaffl 2001). Statistical analysis was performed using Student's t-test; statistical significance was assumed at $p < 0.05$.

Western blotting

Protein extraction and Western blotting from frozen samples was performed as recently described (Braeuning et al. 2011) using antibodies against phosphorylated (pS217/S221) MEK1/2 (Cell Signaling #9154; 1:1,000), ERK1/2 (Cell Signaling #9102; 1:1,000), phosphorylated (pT202/Y204) ERK1/2 (Cell Signaling #4376; 1:1,000), CYP2B and CYP2C (both gift by Dr. R. Wolf; 1:500), and ACTB (β-actin; Sigma #1978; 1:8,000; loading control). For paraffin-embedded, Carnoy-fixed tissue, 3-5 mg of a sample were heated to 95°C in 40 µl lysis buffer (26.7 µl 2xLDS Sample Buffer, 13.3 µl Sample Reducing Agent; both from Invitrogen) for 15 min and, after adding of 40 µl additional lysis buffer, for another 10 min. Molten paraffin was separated from the aqueous phase by centrifugation. Protein determination was performed using the BCA assay in iodoacetamide-treated aliquots.

Reverse-phase protein microarray (RPPA)

RPPA profiling of tumors was performed as previously described (Braeuning et al. 2011). Frozen liver tissue (50-80 mg) was ground under liquid nitrogen and lysed with CLB1 lysis buffer (Bayer Technology Services, Leverkusen, Germany). Protein

concentration of the lysate was determined by the Bradford assay and adjusted to 0.4 mg/ml. RPPAs were printed as described by (Pirnia et al. 2009). Detection of proteins was performed using a two-step immunoassay (antibodies listed in Supplementary Table 1) and Alexa647-labeled secondary antibodies (Invitrogen). Images of the microarrays were taken and analyzed using the ZeptoREADER microarray imager (Bayer Technology Services) and ZeptoVIEW Pro 3.0 software. The weighted mean of replicate sample spots was used for statistical analysis; standard deviation was calculated according to standard error propagation rules from the standard deviations of raw and blank signals. For statistical analysis and graphical representation of the data, MEV 4.8.1 software (Saeed et al. 2006) was used. Hierarchical clustering (Euclidian distance, complete linkage) of median-centred and $\log_2$-transformed data was performed to visualize the differences.

Results

As expected (Aydinlik et al. 2001; Braeuning et al. 2014; Jaworski et al. 2005), DEN treatment of mice yielded GS-negative, basophilic and CDH1-positive hepatocellular adenoma, indicative of MAPK activation by *Ha-ras* or *B-raf* mutations (not shown). The CAR activator PB was administered to the tumor-bearing mice to test for the responsiveness of tumor tissue to stimulation by an exogenous signal.

Surprisingly, some tumors from PB-treated animals exhibited pronounced immunoreactivity for CYP2B and CYP2C, while others did not. *Ha-ras* and *B-raf* mutation analyses revealed that PB-treated tumors with activated Ha-ras expressed lower levels of the CAR target enzyme CYP2B than tumors with activated B-raf (Figure 1A). This was similarly observed for the CAR target mRNAs *Cyp2b10*, *Cyp2c*, *Gstm2*, and *Gstm3* (Figure 1B) and confirmed at the protein level (Supplemental Figure 2). CAR mRNA levels were similarly reduced in both tumor types (Supplemental Figure 3).

Phosphorylation/dephosphorylation plays a substantial role in the regulation of CAR activity (Mutoh et al. 2013). We therefore conducted an RPPA analysis of *Ha-ras*- and *B-raf*-mutated tumors to analyze the phosphorylation of kinases involved in MAPK signaling and/or CAR regulation. Cluster analysis well separated normal liver from the tumors, while separation of tumor genotypes was not consistent (Figure 2). Both tumor types were similarly characterized by their previously known lack of GS and RHBG (Jaworski et al. 2007) and elevated CDH1 levels (Hailfinger et al. 2006).

The phosphorylated isoforms of numerous proliferation- and/or survival-related kinases were altered in the tumors generally showing hyperphosphorylation (Figure 2A). Certain phosphorylated, active kinases were present at especially high levels in *Ha-ras*-mutated tumors, while the levels in *B-raf*-mutated tumors were lower (Figure 2). Clustering only based on the active, phosphorylated versions of ERK1/2, ribosomal S6 kinase (RSK) 1, MAPK kinase (MEK) 1/2, and Jun N-terminal kinase (JNK) 1/2, separated the vast majority of tumors with activating *Ha-ras* mutations from normal liver samples and *B-raf*-mutated tumors by their high levels of these phospho-proteins (Figure 2B). Preferential kinase activation in *Ha-ras*-mutated tumors was verified by immunohistochemistry (Figure 2C) and Western blotting (Figure 2D; Supplemental Figure 2). Immunohistochemically stained tumors were classified into tumors positive or negative for phosphorylated active ERK1/2 and correlated to CYP2B levels. Phospho-ERK-positive tumors generally exhibited weaker staining for CYP2B than their phospho-ERK-negative or only weakly phospho-ERK-positive counterparts (Figure 2E-F).

Discussion

We show that mouse liver adenoma with activating mutations in *Ha-ras* or *B-raf* differ in their activation of kinases from the MAPK pathway. This was unexpected since previous analyses did not reveal remarkable differences between the gene or protein expression profiles of the two tumor types (Jaworski et al. 2007; Rignall et al. 2009). Ha-ras and B-raf activation are similarly believed to activate downstream MAPK signaling, including the kinases that were now found to be differentially activated (Rubinfeld and Seger 2005). The data altogether suggest that the downstream consequences of MAPK activation must be very similar in these tumors, despite considerable differences in the phosphorylation state of the engaged kinases. These results question the frequent use of ERK1/2 phosphorylation as a surrogate marker for the biological activity of the MAPK pathway.

In addition to differences in kinase signaling, our study revealed a differential response of tumors with either *Ha-ras* or *B-raf* mutations to stimulation with a CAR activator: *B-raf*-mutated tumors responded with pronounced induction of CAR target genes similar to normal tissue, whereas induction was weak in *Ha-ras*-mutated tumors. This was also unexpected given the known similarity of the two tumor types (Jaworski et al. 2007; Rignall et al. 2009). Interestingly, kinase activation data provide

a possible explanation for the differential behavior of the two tumor sub-populations: ERK1/2 activation inhibits CAR-dependent transcription by retaining the receptor in the cytosol (Koike et al. 2007). Thus, the strong ERK phosphorylation in *Ha-ras*-mutated tumors may explain the diminished response to CAR activation. Unfortunately, commercially available CAR antibodies did not allow for sufficiently specific immunostaining in order to verify this hypothesis by demonstrating preferential CAR translocation in *B-raf*-mutated tumors. It appears unlikely that variations in the levels of CAR are the cause for the observed differences: Both tumor types show similarly reduced CAR mRNA levels, while *B-raf*-mutated tumors still exhibit substantial CAR target gene induction comparable to normal tissue. Even though no data are available for other CAR agonists or for other species, one might speculate that similar results would be produced with different CAR activators also in other strains or species.

Of note, PB inhibits the outgrowth of MAPK-activated hepatocytes to manifest tumors, when DEN injection is followed by chronic PB treatment (Lee 2000; Moennikes et al. 2000). We assessed tumor multiplicity, tumor volume and BrdU incorporation as a surrogate for cell proliferation to determine whether the administration of PB at a later time point would still have a similar inhibitory effect. However, PB treatment did not affect the aforementioned parameters; as compared to non-PB-treated tumors obtained under otherwise identical experimental conditions (own unpublished data). This indicates that PB might not inhibit the growth of manifest mouse liver adenoma with activated MAPK signaling.

In summary, the present study improves our knowledge on the state of kinase signaling in chemically induced mouse liver tumors and furthermore demonstrates that otherwise very similar tumor sub-populations might react strikingly different when the tumor cells are exposed to a xenobiotic activator of the nuclear receptor CAR.

Acknowledgments

Technical assistance by Johanna Mahr and Elke Zabinsky is acknowledged. We thank Dr. R. Wolf (Dundee, UK) for the gift of CYP antibodies.

Author contributions

Participated in research design: Templin, Schwarz, Braeuning

Conducted experiments: Kollotzek, Knorpp, Braeuning

Performed data analysis: Zeller, Knorpp, Templin, Braeuning

Wrote the paper: Braeuning, Schwarz

References

Aydinlik H, Nguyen TD, Moennikes O, Buchmann A, Schwarz M (2001) Selective pressure during tumor promotion by phenobarbital leads to clonal outgrowth of beta-catenin-mutated mouse liver tumors. Oncogene 20(53):7812-6 doi:10.1038/sj.onc.1204982

Braeuning A, Bucher P, Hofmann U, Buchmann A, Schwarz M (2014) Chemically induced mouse liver tumors are resistant to treatment with atorvastatin. BMC cancer 14:766 doi:10.1186/1471-2407-14-766

Braeuning A, Heubach Y, Knorpp T, et al. (2011) Gender-specific interplay of signaling through beta-catenin and CAR in the regulation of xenobiotic-induced hepatocyte proliferation. Toxicological sciences : an official journal of the Society of Toxicology 123(1):113-22 doi:10.1093/toxsci/kfr166

Braeuning A, Schwarz M (2010) Zonation of heme synthesis enzymes in mouse liver and their regulation by beta-catenin and Ha-ras. Biological chemistry 391(11):1305-13 doi:10.1515/BC.2010.115

Braeuning A, Singh Y, Rignall B, et al. (2010) Phenotype and growth behavior of residual beta-catenin-positive hepatocytes in livers of beta-catenin-deficient mice. Histochemistry and cell biology 134(5):469-81 doi:10.1007/s00418-010-0747-1

Elcombe CR, Peffer RC, Wolf DC, et al. (2014) Mode of action and human relevance analysis for nuclear receptor-mediated liver toxicity: A case study with phenobarbital as a model constitutive androstane receptor (CAR) activator. Critical reviews in toxicology 44(1):64-82 doi:10.3109/10408444.2013.835786

Hailfinger S, Jaworski M, Braeuning A, Buchmann A, Schwarz M (2006) Zonal gene expression in murine liver: lessons from tumors. Hepatology 43(3):407-14 doi:10.1002/hep.21082

Hernandez JP, Mota LC, Baldwin WS (2009) Activation of CAR and PXR by Dietary, Environmental and Occupational Chemicals Alters Drug Metabolism, Intermediary Metabolism, and Cell Proliferation. Curr Pharmacogenomics Person Med 7(2):81-105 doi:10.2174/187569209788654005

Jaworski M, Buchmann A, Bauer P, Riess O, Schwarz M (2005) B-raf and Ha-ras mutations in chemically induced mouse liver tumors. Oncogene 24(7):1290-5 doi:10.1038/sj.onc.1208265

Jaworski M, Ittrich C, Hailfinger S, et al. (2007) Global gene expression in Ha-ras and B-raf mutated mouse liver tumors. International journal of cancer Journal international du cancer 121(6):1382-5 doi:10.1002/ijc.22801

Knebel C, Neeb J, Zahn E, et al. (2018) Unexpected Effects of Propiconazole, Tebuconazole, and Their Mixture on the Receptors CAR and PXR in Human Liver

Cells. Toxicological sciences : an official journal of the Society of Toxicology 163(1):170-181 doi:10.1093/toxsci/kfy026

Kobayashi K, Hashimoto M, Honkakoski P, Negishi M (2015) Regulation of gene expression by CAR: an update. Archives of toxicology 89(7):1045-55 doi:10.1007/s00204-015-1522-9

Koike C, Moore R, Negishi M (2007) Extracellular signal-regulated kinase is an endogenous signal retaining the nuclear constitutive active/androstane receptor (CAR) in the cytoplasm of mouse primary hepatocytes. Molecular pharmacology 71(5):1217-21 doi:10.1124/mol.107.034538

Lee GH (2000) Paradoxical effects of phenobarbital on mouse hepatocarcinogenesis. Toxicologic pathology 28(2):215-25

Loeppen S, Koehle C, Buchmann A, Schwarz M (2005) A beta-catenin-dependent pathway regulates expression of cytochrome P450 isoforms in mouse liver tumors. Carcinogenesis 26(1):239-48 doi:10.1093/carcin/bgh298

Moennikes O, Buchmann A, Romualdi A, et al. (2000) Lack of phenobarbital-mediated promotion of hepatocarcinogenesis in connexin32-null mice. Cancer research 60(18):5087-91

Molnar F, Kublbeck J, Jyrkkarinne J, Prantner V, Honkakoski P (2013) An update on the constitutive androstane receptor (CAR). Drug metabolism and drug interactions 28(2):79-93 doi:10.1515/dmdi-2013-0009

Mutoh S, Sobhany M, Moore R, et al. (2013) Phenobarbital indirectly activates the constitutive active androstane receptor (CAR) by inhibition of epidermal growth factor receptor signaling. Sci Signal 6(274):ra31 doi:10.1126/scisignal.2003705

Oshida K, Vasani N, Jones C, et al. (2015) Identification of chemical modulators of the constitutive activated receptor (CAR) in a gene expression compendium. Nucl Recept Signal 13:e002 doi:10.1621/nrs.13002

Pfaffl MW (2001) A new mathematical model for relative quantification in real-time RT-PCR. Nucleic acids research 29(9):e45

Pirnia F, Pawlak M, Thallinger GG, et al. (2009) Novel functional profiling approach combining reverse phase protein microarrays and human 3-D ex vivo tissue cultures: expression of apoptosis-related proteins in human colon cancer. Proteomics 9(13):3535-48 doi:10.1002/pmic.200800159

Rignall B, Ittrich C, Krause E, Appel KE, Buchmann A, Schwarz M (2009) Comparative transcriptome and proteome analysis of Ha-ras and B-raf mutated mouse liver tumors. Journal of proteome research 8(8):3987-94 doi:10.1021/pr9002933

Rubinfeld H, Seger R (2005) The ERK cascade: a prototype of MAPK signaling. Mol Biotechnol 31(2):151-74 doi:10.1385/MB:31:2:151

Saeed AI, Bhagabati NK, Braisted JC, et al. (2006) TM4 microarray software suite. Methods in enzymology 411:134-93 doi:10.1016/S0076-6879(06)11009-5

Tannenbaum C, Sheehan NL (2014) Understanding and preventing drug-drug and drug-gene interactions. Expert Rev Clin Pharmacol 7(4):533-44 doi:10.1586/17512433.2014.910111

Unterberger EB, Eichner J, Wrzodek C, et al. (2014) Ha-ras and beta-catenin oncoproteins orchestrate metabolic programs in mouse liver tumors. International journal of cancer Journal international du cancer 135(7):1574-85 doi:10.1002/ijc.28798

Wada T, Gao J, Xie W (2009) PXR and CAR in energy metabolism. Trends in endocrinology and metabolism: TEM 20(6):273-9 doi:10.1016/j.tem.2009.03.003

Footnote

This work was supported by the Medical Faculty of the University of Tübingen [fortüne program].

Figure legends

Figure 1. Expression of marker proteins in mouse liver tumors following treatment with the CAR activator PB. **(A)** Tumors with activated Ha-ras and B-raf lack GS and overexpress CDH1. The model CAR target CYP2B is high in *B-raf*-mutated, but not in *Ha-ras*-mutated hepatomas following exposure to PB. Representative images are shown. **(B)** Levels of CAR target mRNAs in normal liver (NL) or tumor tissue with or without PB treatment, as determined by real-time RT-PCR (n ≥ 3 per group). Statistical significance: *, $p < 0.05$, **, $p < 0.01$; Student's t-test.

Figure 2. CAR-dependent protein expression in mouse liver tumors. **(A)** Phospho-proteomic profiling by RPPA, visualized as clustered heat-map. **(B)** Re-clustering on the basis of the activated phospho-forms of selected kinases. Sample designations: N, normal liver; H, *Ha-ras*-mutated tumor; B, *B-raf*-mutated tumor. Up- and downregulation are shown in red and green, respectively. **(C)** Verification of different levels of the phosphorylated active kinases in *Ha-ras*- and *B-raf*-mutated liver tumors. Hematoxylin/eosin staining (H&E), staining for ERK 1/2 pT202/Y204 (pERK), and JNK/SAPK pT183/Y185 (pJNK) is shown. Identified gene mutations are indicated. Enhanced display details from the *Ha-ras*-mutated liver tumor from **(C)** are also presented. Control staining was performed w/o the primary antibody. Abbreviations: n, normal tissue; t, tumor. The scale bar indicates 50 µm. **(D)** Western blotting of tumor tissue protein extracts. Representative blots for the different phosphorylated kinases are comparatively shown for normal liver (NL) and liver tumors harboring activating mutations in either *Ha-ras* (Ras) or *B-raf* (Raf). **(E)** Correlation of PB-induced CYP2B expression, ERK 1/2 phosphorylation status, and mutation status in mouse liver tumors: immunohistochemical staining demonstrating the linkage between ERK 1/2 phosphorylation at T202/Y204 (pERK) and CYP2B expression. Representative images are shown. **(F)** Correlation of ERK 1/2 phosphorylation and CYP2B expression in tumors, as determined by visual grading of staining intensity of CYP2B-immunostained tissue slices, demonstrating the lack of CYP2B induction by PB in tumors with strong phospho-ERK immunoreactivity. Numbers of investigated tumors are indicated in the graph.

Figure 1

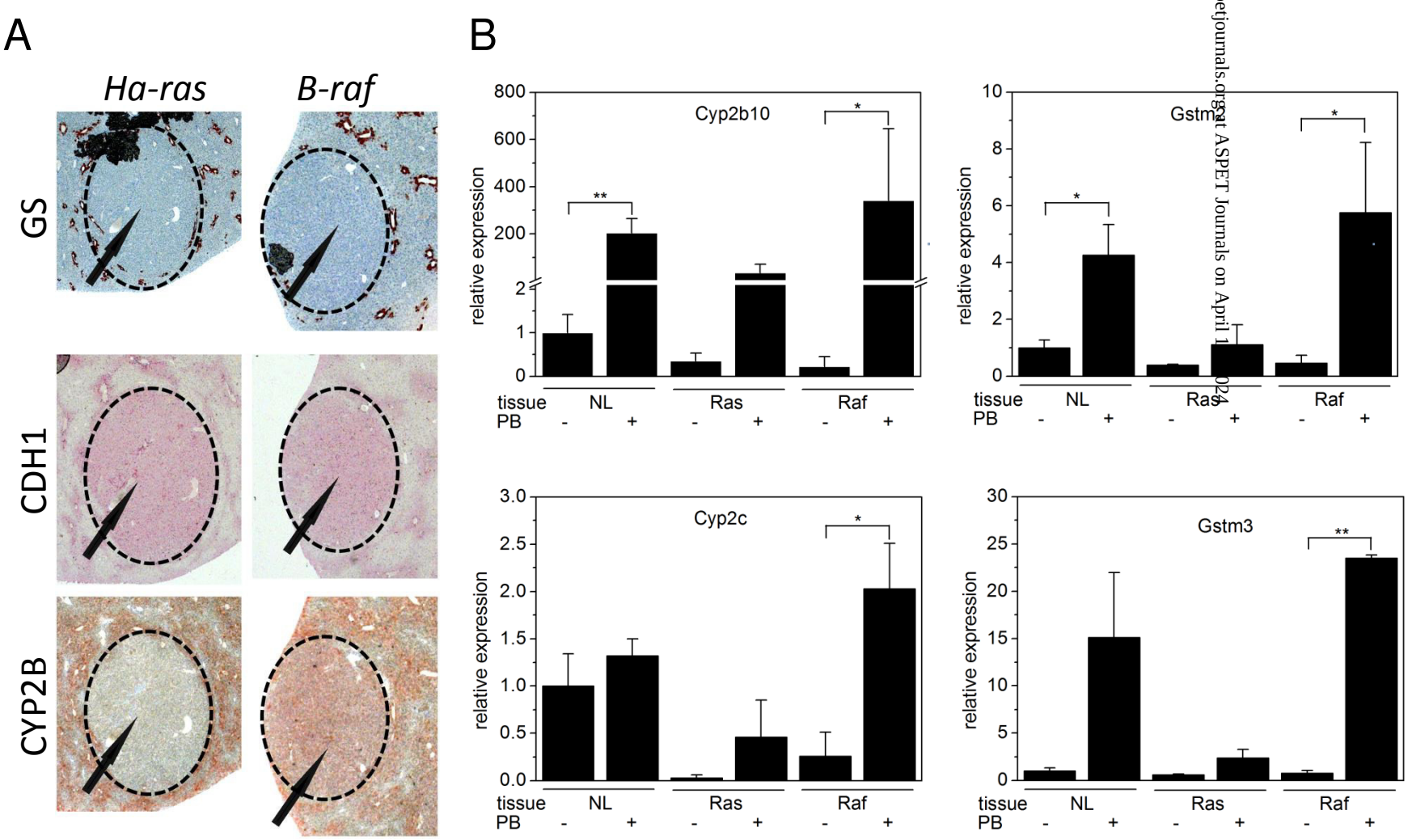

Figure 2

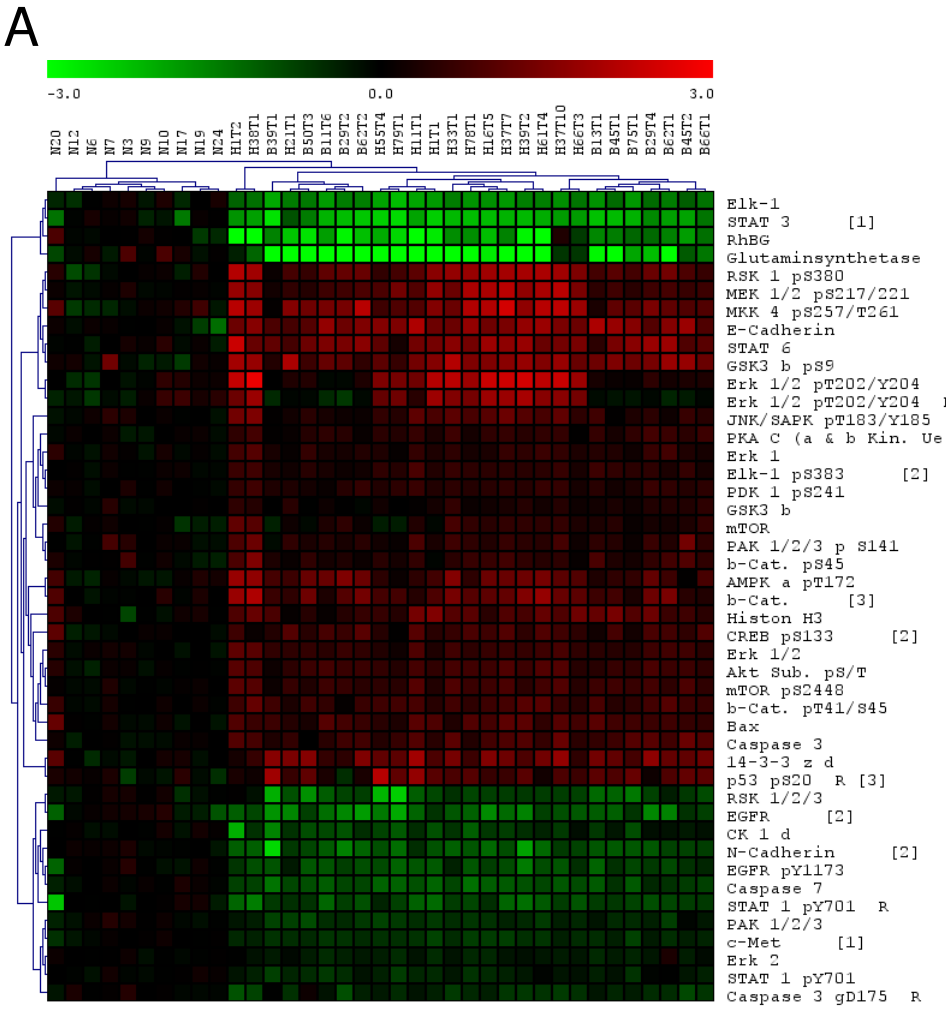

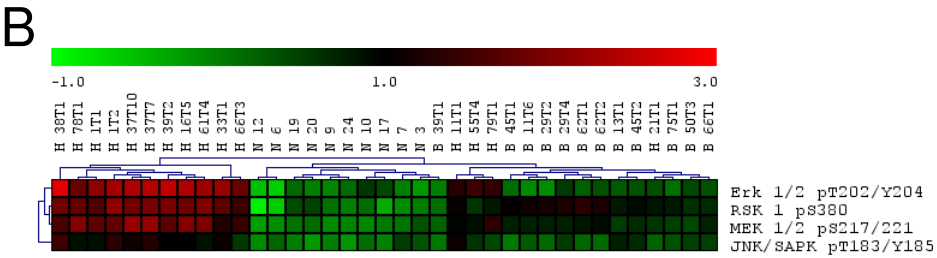

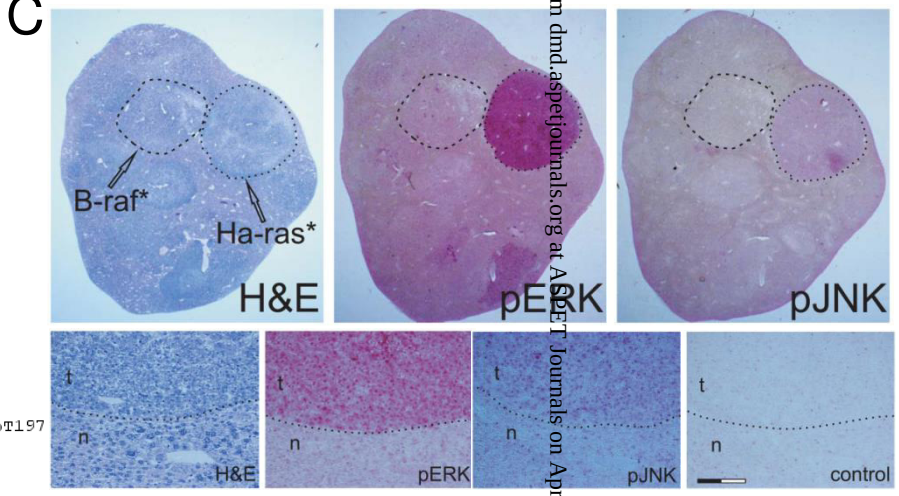

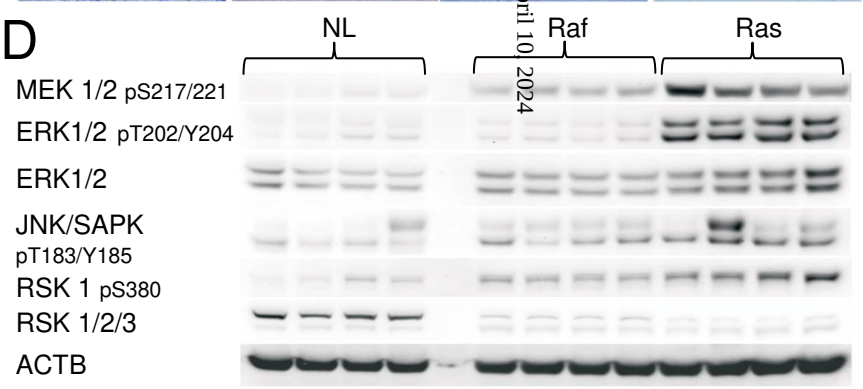

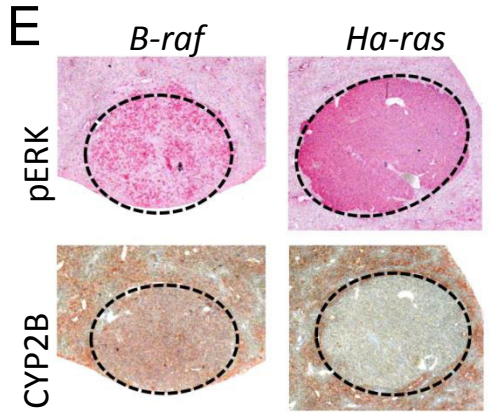

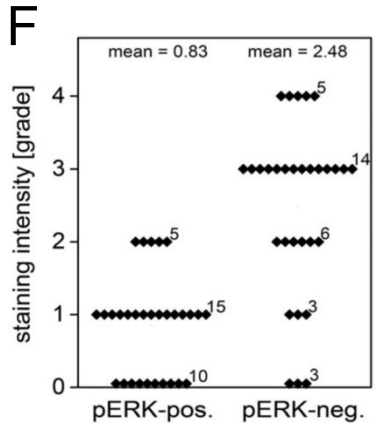

Mouse hepatomas with *Ha-ras* and *B-raf* mutations differ in mitogen-activated protein kinase signaling and response to constitutive androstane receptor activation

Albert Braeuning, Ferdinand Kollotzek, Eva Zeller, Thomas Knorpp, Markus F. Templin, Michael Schwarz

Drug Metabolism and Disposition
DMD # 83014

Content:

Supplemental Figure 1

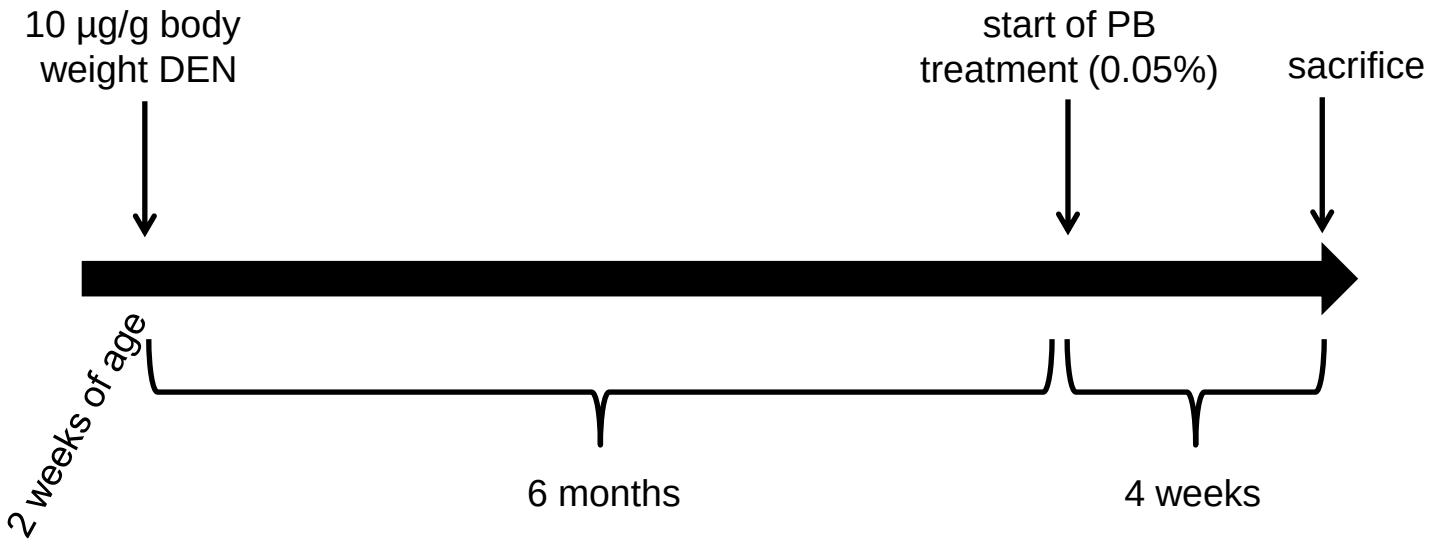

Supplemental Figure 1: Schematic representation (not to scale) of the treatment protocol. Tumor initiation was achieved by a single i.p. injection of diethylnitrosamine (DEN) at 2 weeks of age, followed a by treatment-free interval of 6 months. Then, mice received a diet containing 0.05% (w/w) phenobarbital (PB) for 4 weeks prior to sacrifice.

Supplemental Figure 2

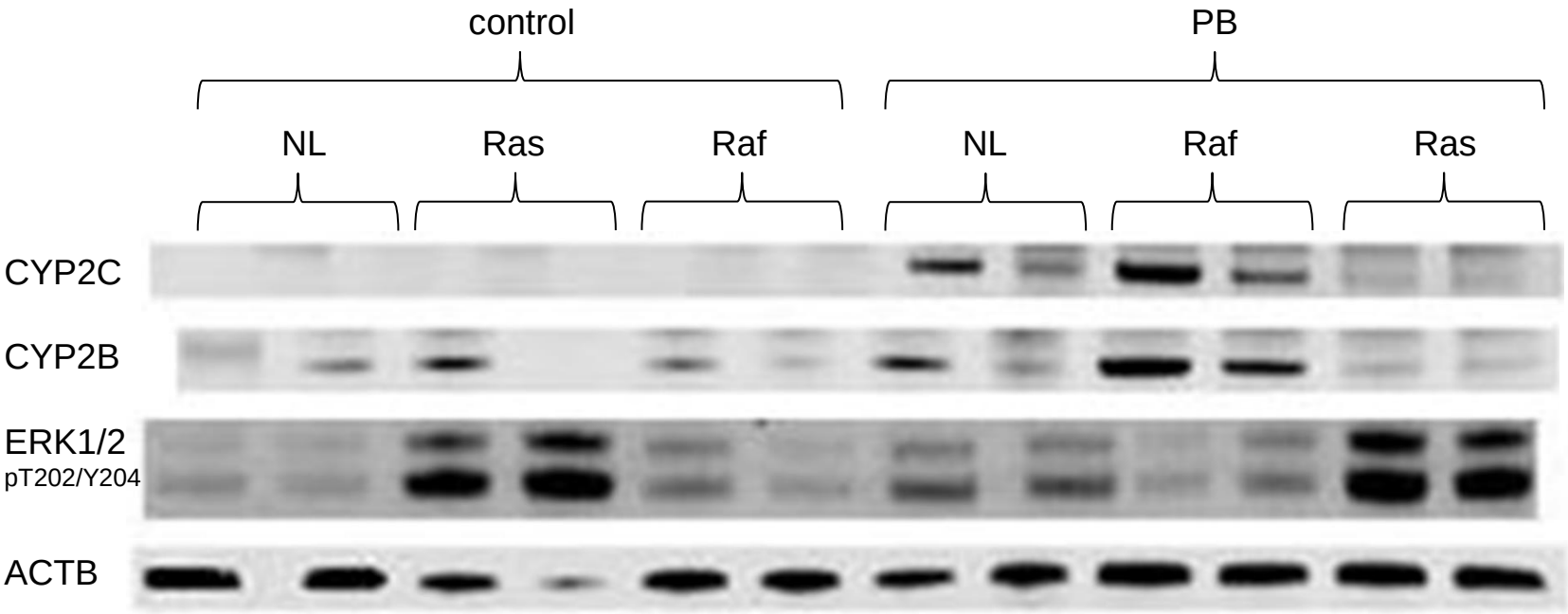

Supplemental Figure 2: Western Blot verification of differential expression of the CAR targets in normal liver (NL) and in mouse liver tumors with activating mutations in either *Ha-ras* (Ras) or *B-raf* (Raf). Analyses of tumors not treated with PB (control) and treated with PB are presented. For each sample type, material from two different tumors is shown. Proteins were isolated from the Carnoy-fixed paraffin-embedded tissue blocks also used for immunostaining and mutation analysis. Western blot images for the cytochrome P450 enzymes CYP2C, CYP2B, as well as for the phosphorylated active version of extracellular signal-regulated kinase (ERK) 1/2 are shown. Treatment of tissue with phenobarbital (PB) is indicated. Beta-actin (ACTB) was used as a loading control. Material from the same paraffin-embedded tissue blocks also used for immunohistochemical staining and mutation analysis was used for Western blotting.

Supplemental Figure 3

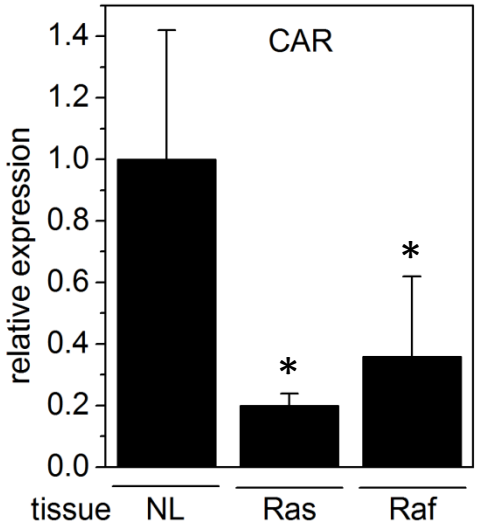

Supplemental Figure 3: CAR mRNA levels in normal liver (NL) and mouse liver tumors with activating mutations in either *Ha-ras* (Ras) or *B-raf* (Raf). Mean +SD (n≥5) is given relative to normal liver tissue. Statistical significance: *, $p < 0.05$, Student‘s t-test.

Supplementary Table 1

Supplementary Table 1: Antibodies used for RPPA assay.

Antigen	Supplier
14-3-3 ζ δ	Cell Signalling Technologies
Akt Substrate - phospho S/T	Cell Signalling Technologies
AMPK α - phospho T172	Cell Signalling Technologies
Bax	Cell Signalling Technologies
Caspase 3	Cell Signalling Technologies
Caspase 3 - gespalten D175	Cell Signalling Technologies
Caspase 7	Cell Signalling Technologies
CK 1 δ	kind gift by Prof. U. Knippschild, Universität Ulm
c-Met [1]	R&D Systems
CREB - phospho S133 [2]	Cell Signalling Technologies
E-Cadherin	R&D Systems
EGFR [2]	Epitomics
EGFR - phospho Y1173	Biomol
Elk-1	Cell Signalling Technologies
Elk-1 - phospho S383 [2]	R&D Systems
Erk 1	Cell Signalling Technologies
Erk 1/2	Cell Signalling Technologies
Erk 1/2 - phospho T202/Y204	Cell Signalling Technologies
Erk 2	Cell Signalling Technologies
Glutaminsynthetase	Sigma-Aldrich
GSK3 β	Cell Signalling Technologies
GSK3 β - phospho S9	Cell Signalling Technologies
Histon H3	Cell Signalling Technologies
JNK/SAPK - phospho T183/Y185	Cell Signalling Technologies
MEK 1/2 - phospho S217/221	Cell Signalling Technologies
MKK 4 - phospho S257/T261	Cell Signalling Technologies
mTOR	Cell Signalling Technologies
mTOR - phospho S2448	Cell Signalling Technologies
N-Cadherin [2]	BD Biosciences
p53 [3]	R&D Systems
p53 - phospho S20	Cell Signalling Technologies
PAK 1/2/3	Cell Signalling Technologies
PAK 1/2/3 - phospho S141	Invitrogen
PDK 1 - phospho S241	Cell Signalling Technologies
PKA C (α & β Kinase Untereinheit) - phospho T197	Invitrogen
RhBG	kind gift by Dr. R. Chambrey, INSERM, Paris
RSK 1 - phospho S380	Cell Signalling Technologies
RSK 1/2/3	Cell Signalling Technologies
STAT 1	Cell Signalling Technologies
STAT 1 - phospho Y701	Cell Signalling Technologies
STAT 3 [1]	Cell Signalling Technologies
STAT 6	Cell Signalling Technologies
β-Actin	Sigma-Aldrich
β-Catenin [3]	Invitrogen
β-Catenin - phospho S45	Cell Signalling Technologies
β-Catenin - phospho T41/S45	Cell Signalling Technologies